Few-Body Syst (2018) 59:90
https://doi.org/10.1007/s00601-018-1406-7

Ioana Niculescu

Quark Hadron Duality in Unpolarized Structure Functions

Received: 4 January 2018 / Accepted: 14 May 2018
© Springer-Verlag GmbH Austria, part of Springer Nature 2018

Abstract Quark hadron duality establishes an intriguing connection between medium and high energy physics by identifying, in certain cases, dual descriptions of observables either in terms of explicit quark degrees of freedom or as averages over hadronic variables. Duality has been studied extensively in inclusive electron scattering experiments at Jefferson Lab. The present talk is an overview of these results for unpolarized structure functions for proton, neutron, and nuclei.

1 Introduction

Understanding the nucleon structure has been an important goal of nuclear and particle physics research. Parton distribution functions (PDFs) are used to describe the quark localization inside the nucleon and inclusive electron scattering provides some of the data needed to extract these PDFs.

In order to probe the quark structure of the nucleon the wavelength of the virtual photon probe should be small. In this case the lepton–nucleon interaction can be viewed as the incoherent scattering of the virtual photon from a single quark. As the four-momentum transfer squared Q^2 decreases, initial and final state interactions between the struck quark and the remnants of the target must be included in the description of the interaction. In the first case, perturbative QCD describes the data well, while in the second non-perturbative effects have to be taken into account. This transition from the perturbative to the non-perturbative regime is of great interest in the field.

The inclusive electron scattering cross section can be written in terms of two structure functions: $xF_1(x, Q^2)$ and $F_2(x, Q^2)$, which can be related to the quark and anti-quark distribution functions:

$$\frac{d^2\sigma}{dE'd\Omega} = \frac{8\alpha^2\cos^2(\theta/2)}{Q^4}\left[\frac{F_2\left(x, Q^2\right)}{\nu} + \frac{2F_1\left(x, Q^2\right)}{M}\tan^2\left(\theta/2\right)\right]. \tag{1}$$

Here $x = Q^2/2M\nu$ is the Bjorken scaling variable, M is the proton mass, $\nu = E - E'$ is the virtual photon energy in the target rest frame, and E and E' are the incident and scattered electron energies, respectively.

At high enough energies the cross section can be modeled just by taking into account the quark and gluon degrees of freedom. As the energy decreases, resonance production, a highly non-perturbative effect, becomes more important. Quark–hadron duality reflects the relationship between the quark and hadron descriptions of hadronic processes.

This article belongs to the Topical Collection “NSTAR 2017 - The International Workshop on the Physics of Excited Nucleons”.

I. Niculescu (✉)
James Madison University, Harrisonburg, VA 22807, USA
E-mail: niculemi@jmu.edu

Published online: 04 June 2018

In the framework of QCD quark–hadron duality can be interpreted using structure function moments, defined as integrals of the structure function:

$$M_n(Q^2) = \int_0^1 x^{n-2} F\left(x, Q^2\right) dx \tag{2}$$

where n is the order of the moment. These moments can be expanded as a series in $1/Q^2$ (operator product expansion or OPE) with the leading-twist term corresponding to the incoherent scattering of the virtual photon from a single parton. The higher twist terms which have higher powers of $1/Q^2$ correspond to processes in which the struck parton interacts with the other partons and gluons in the nucleon. De Rujula et al. [1] explained the quark–hadron duality phenomenon observed experimentally by Bloom and Gilman [2,3] as a suppression of higher twists, which occurs if the interaction between the struck quark and the spectator system is minimized.

2 Quark–Hadron Duality for the Proton

Quark–hadron duality was first observed by Bloom and Gilman in the 1970s using inclusive electron-proton scattering measurements from SLAC. The availability of a medium energy, high duty factor, high luminosity electron beam at Jefferson Lab has allowed a much more in depth study of duality both for unpolarized and polarized proton structure functions.

A sample of proton F_2 structure function data [4] is shown in Fig. 1 as a function of $W^2 = M^2 + 2M\nu - Q^2$, the invariant mass squared of the final hadronic state. The scaling curve shown was obtained by averaging all the nucleon resonance F_2 data as described in [5]. It is observed that the three prominent resonances do not disappear relative to the background under them as the four-momentum transfer squared increases but fall at roughly the same rate. Also, the structure function in the resonance region ($W \leq 2$) roughly averages to the scaling limit function F_2.

The Cornwall–Norton moments of F_2 [Eq. (2)] can be used to quantitatively investigate duality. To be able to calculate the integral which extends from $x = 0$ to $x = 1$ data from other available experiments (ZEUS, NMC, SLAC) were included, as described in [6]. The results for the first four Cornwall–Norton moments ($n = 2, 4, 6, 8$) are shown in Fig. 2. The solid line represents the contribution of the elastic peak, which dominates at lower Q^2. The dashed lines are the moments at higher Q^2 which were extracted using parameterizations of world's inclusive electron–proton scattering data.

It should be noted that the Q^2 dependence of the moments at small Q^2 is mainly dictated by the elastic peak, a highly non-perturbative effect. This behavior is to be expected if one takes into account the dramatic decrease of the elastic cross section with increasing Q^2. However, if the contribution of the elastic peak is not included, the data presented in [6] exhibit duality even for very low Q^2, supporting the hypothesis that the higher twist contributions are on average reduced in the nucleon resonance region even for $Q^2 \simeq 1\ \mathrm{GeV}^2$. This does not, however, preclude the existence of sizeable higher twist effects if much smaller kinematic regions are considered; obviously, duality is not observed in the limited region on top of any given resonance peak. Similar results were obtained for the separated proton structure functions F_1 and F_L [7,8].

3 Quark–Hadron Duality for Nuclei

Studies of nuclear structure functions have revealed additional insight into the quark–hadron duality phenomenon. Using high x, lower Q^2 data from Jefferson Lab in addition to other available data sets, the Cornwall–Norton moments of F_2^A were constructed [9]:

$$M_n\left(Q^2\right) = \int_0^A x^{n-2} F\left(x, Q^2\right) dx \tag{3}$$

The second moment ($n = 2$) of F_2 for the proton, deuteron, and iron are shown in Fig. 3. The empty circles represent an extraction of the neutron moments using the difference between the deuteron and proton data:

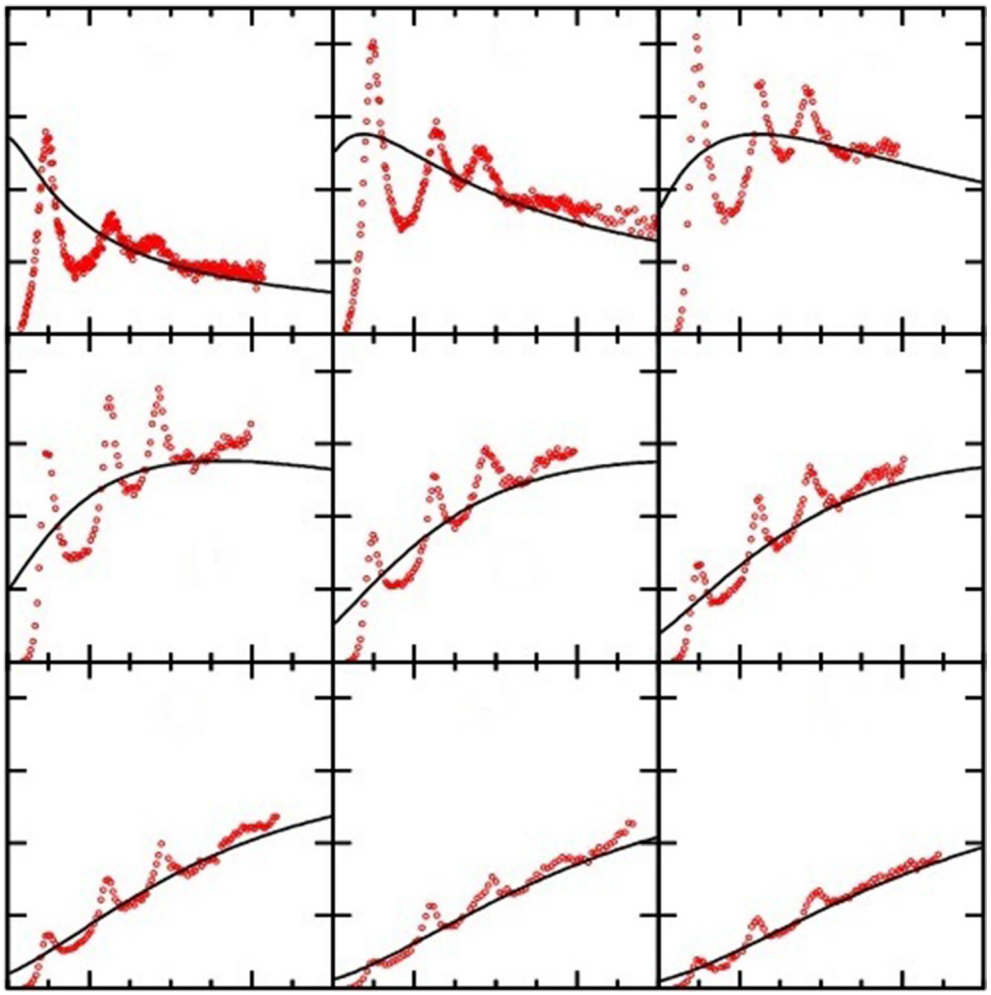

Fig. 1 Proton F_2 structure function data as a function of W^2. Each panel is at a different Q^2: 0.07, 0.2, 0.45, 0.82, 1.40, 1.70, 2.40, 3.00, and 3.30 GeV^2. The lowest two Q^2 data sets are from an older SLAC experiment, while all the other data are from Jefferson Lab. The scaling curve shown is the duality averaged curve obtained in [5]

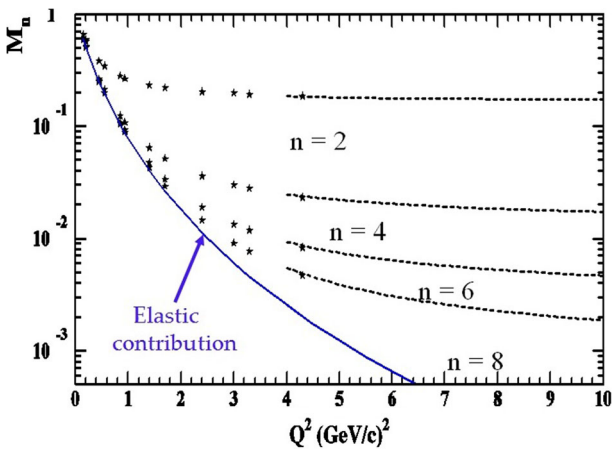

Fig. 2 Proton Cornwall–Norton moments for $n = 2, 4, 6, 8$ as a function of Q^2. The solid line represents the elastic contribution

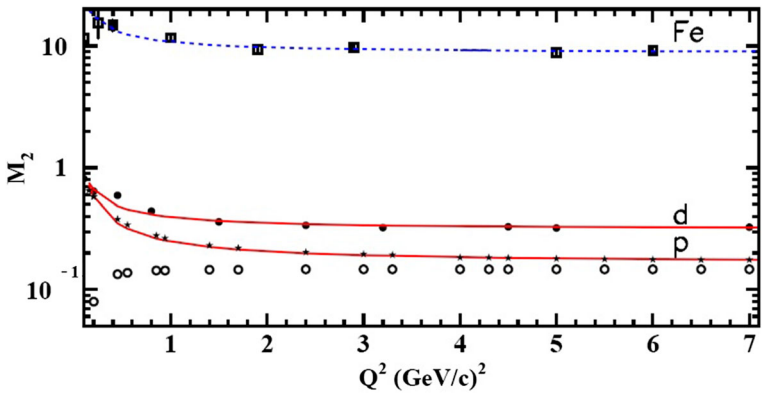

Fig. 3 Proton (stars), deuteron (full circles), and iron (squares) Cornwall–Norton moments as a function of Q^2. The open circles represent the difference between the deuterium and proton moments. The solid lines are obtained by fitting the moments for proton and deuteron, and using the procedure described in the text for iron

$M_2(n) = M_2(d) - M_2(p)$. If the nuclear effects are small, the Cornwall–Norton moments for iron can be calculated using the proton and neutron data:

$$M_2(Fe) = Z \times M_2(p) + (A - Z) \times M_2(n) \tag{4}$$

where $M(p)$, $M(n)$, and $M(Fe)$ represent the proton, neutron, and iron moments, respectively. This extraction is shown as a dashed line in Fig. 3. This somewhat naive result agrees well with the moments obtained directly from Fe data. This was interpreted in [9] as evidence for very small nuclear effects due to cancellations between shadowing, antishadowing, and EMC regions.

4 Quark–Hadron Duality for the Neutron

In addition to the studies described above for the proton and nuclei, quark–hadron duality was investigated for the neutron [10,11]. In the absence of a free neutron target all information about the neutron has to be extracted from deuterium. A new experimental technique based on spectator proton tagging was used at Jefferson Lab to access the free neutron structure function [12]. By detecting the low momentum backward moving spectator protons the BONuS experiment [13,14] extracted F_2^n with minimal uncertainty from nuclear smearing and nuclear re-scattering corrections.

The kinematic coverage of the BONuS experiment did not allow calculations of the Cornawll–Norton moments given in Eq. (2). Therefore, truncated moments were used for quark–hadron duality studies [15]:

$$M_n\left(x_{min}, x_{max}, Q^2\right) = \int_{x_{min}}^{x_{max}} x^{n-2} F\left(x, Q^2\right) dx \tag{5}$$

The values x_{min} and x_{max} are chosen to correspond to the three prominent resonance regions: the Δ resonance region ($1.3 \leq W^2 \leq 1.9$ GeV^2), the second resonance region ($1.9 \leq W^2 \leq 2.5$ GeV^2) and the third resonance region ($2.5 \leq W^2 \leq 3.1$ GeV^2).

These truncated moments were compared to similar quantities obtained using the ABKM global PDF parameterization [16]. Figure 4 shows this comparison for the second moment ($n = 2$) as a function of Q^2. The four panels correspond to the three resonance regions, while the fourth panel shows the whole resonance region ($1.3 \leq W^2 \leq 4.0$ GeV^2). The fact that this ratio is close to unity indicates that local quark–hadron duality holds for the neutron with the exception of the first resonance region where the model underestimates the data by 20–30%. The model-dependent analysis of Malace et al. [10] are also shown in Fig. 4 and is in good agreement with the present data.

In this kinematic regime the finite-Q^2 corrections (target mass and higher twist effects) are important. To illustrate this ratios of the moments calculated from the CTEQ–Jefferson Lab (CJ) global PDF parametrization [17] with and without higher twist corrections to the full ABKM moments are shown in Fig. 4. This ratio is close to unity over the entire range of Q^2 considered when both parameterizations include finite-Q^2 effects.

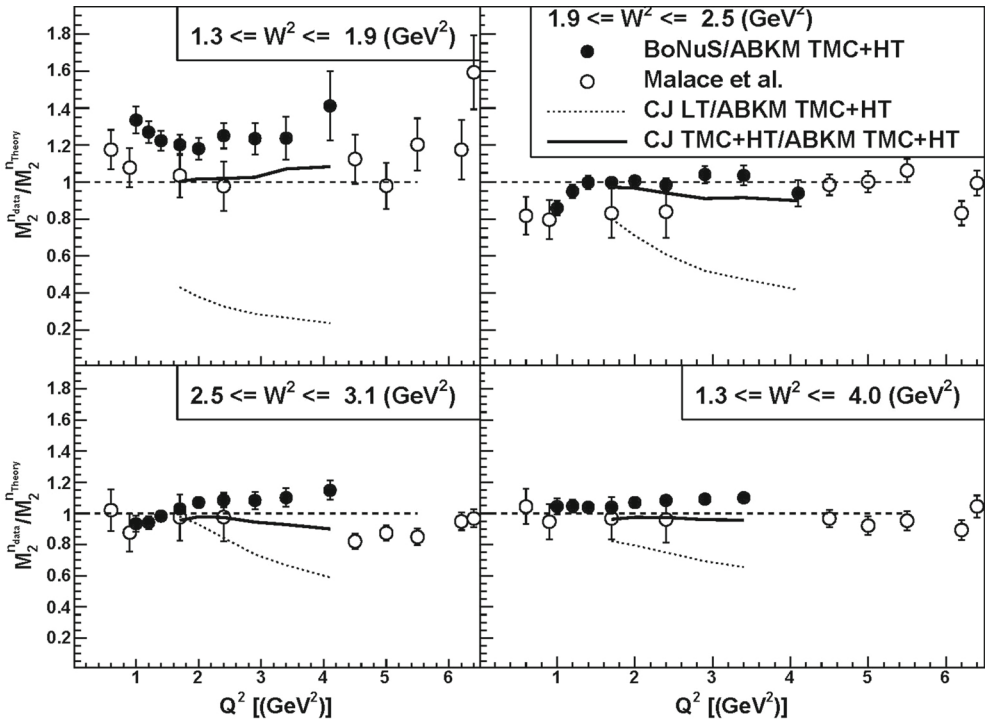

Fig. 4 Ratio of the neutron truncated moments extracted using the BONuS data and the same quantity obtained from the ABKM parameterization. The open circles correspond to the model-dependent extraction of [10]. The dotted and solid lines are ratios computed using the CJ12 parameterization

However, there are significant (30–40%) deviations when only the leading twist components of the CJ fit were used to calculate the moments. These deviations were up to twice as much for the Δ resonance region. Therefore, the finite-Q^2 corrections to the scaling functions play an important role in the cancellations between the individual resonance regions which are necessary for the realization of quark–hadron duality.

The confirmation of local duality for the neutron suggests a dynamical origin of duality and that the phenomenon is not accidental, but is a general property of nucleon structure functions.

5 Future Quark–Hadron Duality Studies at Jefferson Lab

One of the first experiments in Hall C at Jefferson Lab after the energy upgrade will be experiment E12-10-002 [18]. This experiment will measure the spin averaged proton and deuteron structure functions in the resonance region and beyond up to x of 0.99 and Q^2 of 17 GeV^2. This will extend the kinematic coverage and will enable further studies of quark–hadron duality.

In the future, the spectator tagging technique will be used at Jefferson Lab with an 11 GeV electron beam to extend the kinematic coverage of the neutron structure function F_2^n measurements to higher values of x, up to 0.8, and Q^2, up to 14 GeV^2 [19]. These data will provide more stringent constraints on the leading twist PDFs in the limit $x \to 1$, as well as allowing more definitive tests of local quark–hadron duality for the neutron over a greater range of Q^2.

6 Conclusion

In conclusion, this paper summarizes important results in quark–hadron duality studies: duality in inclusive electron scattering off the proton, the neutron, as well as off heavier nuclei. In all cases duality seems to hold globally as well as locally, suggesting that it is a fundamental property of nucleons and nuclei. Future experiments will help shed light on the origin of quark–hadron duality by extending the kinematic coverage for F_2, as well as investigate duality in other structure functions and in other processes.

Acknowledgements Funding was provided by National Science Foundation Division of Physics (Grant No. 1614475).

References

1. A. De Rujula, H. Georgi, H.D. Politzer, Ann. Phys. **103**, 315 (1975)
2. E.D. Bloom, F.J. Gilman, Phys. Rev. Lett. **25**, 1140 (1970)
3. E.D. Bloom, F.J. Gilman, Phys. Rev. D **4**, 2901 (1971)
4. I. Niculescu et al., Phys. Rev. Lett. **85**, 1186 (2000)
5. I. Niculescu et al., Phys. Rev. Lett. **85**, 1182 (2000)
6. C. Armstrong et al., Phys. Rev. D **63**, 094008 (2001)
7. Y. Liang et al., JLAB-PHY-04-45 (2004), submitted to Phys. Rev. Lett
8. P. Monaghan, A. Accardi, M.E. Christy, C.E. Keppel, W. Melnitchouk, L. Zhu, Phys. Rev. Lett. **110**, 152002 (2013)
9. I. Niculescu, J. Arrington, R. Ent, C. Keppel, Phys. Rev. C **73**, 035205 (2006)
10. S. Malace, Y. Kahn, W. Melnitchouk, C.E. Keppel, Phys. Rev. Lett. **104**, 102001 (2010)
11. I. Niculescu et al., Phys. Rev. C **91**, 055206 (2015)
12. H. Fenker et al., Nucl. Instrum. Methods A **592**, 273 (2008)
13. N. Baillie et al., Phys. Rev. Lett. **108**, 199902 (2012)
14. S. Tkachenko et al., Phys. Rev. C **89**, 045206 (2014)
15. A. Psaker, W. Melnitchouk, M.E. Christy, C. Keppel, Phys. Rev. C **78**, 025206 (2008)
16. S. Alekhin, J. Blumlein, S. Klein, S. Moch, Phys. Rev. D **81**, 014032 (2010)
17. J.F. Owens, W. Melnitchouk, A. Accardi, Phys. Rev. D **87**, 094012 (2013)
18. Jefferson Lab Experiment E12-10-002, S. Malace, M. Christy, C. Keppel, M. Niculescu, spokespersons
19. Jefferson Lab Experiment E12-10-102, S. Bultmann, M.E. Christy, H. Fenker, K. Griffioen, C.E. Keppel, S. Kuhn, W. Melnitchouk, spokespersons